

Citation for published version:
Mattia, D, Jones, M, O'Byrne, J, Griffiths, O, Owen, R, Sackville, E, McManus, M & Plucinski, P 2015, 'Towards Carbon Neutral CO2 Conversion to Hydrocarbons', *ChemSusChem*, vol. 8, no. 23, pp. 4064-4072. https://doi.org/10.1002/cssc.201500739

DOI:

10.1002/cssc.201500739

Publication date: 2015

Document Version Early version, also known as pre-print

Link to publication

This is the peer reviewed version of the following article: Mattia, D, Jones, M, O'Byrne, J, Griffiths, O, Owen, R, Sackville, E, McManus, M & Plucinski, P 2015, 'Towards Carbon Neutral CO2 Conversion to Hydrocarbons' ChemSusChem, vol 8, no. 23, pp. 4064-4072, which has been published in final form at http://dx.doi.org/0.1002/cssc.201500739 . This article may be used for non-commercial purposes in accordance with Wiley Terms and Conditions for Self-Archiving.

University of Bath

Alternative formats

If you require this document in an alternative format, please contact: openaccess@bath.ac.uk

Copyright and moral rights for the publications made accessible in the public portal are retained by the authors and/or other copyright owners and it is a condition of accessing publications that users recognise and abide by the legal requirements associated with these rights.

Take down policyIf you believe that this document breaches copyright please contact us providing details, and we will remove access to the work immediately and investigate your claim.

Download date: 09 Mar 2023

Towards Carbon Neutral CO₂ Conversion to Hydrocarbons

Davide Mattia, *^[a] Matthew D. Jones, *^[b] Justin P. O'Byrne, ^[a] Owen G. Griffiths, ^[c] Rhodri E. Owen, ^[b] Emma Sackville, ^[a] Marcelle McManus, ^[c] Pawel Plucinski. ^[a]

Abstract: With fossil fuels still predicted to contribute close to 80% of the primary energy consumption by 2040, methods to limit further carbon dioxide emissions in the atmosphere are urgently needed to avoid the catastrophic scenarios associated with global warming. In parallel with improvements in energy efficiency and CO₂ storage, the conversion of CO2 has emerged as a complementary route with significant potential. In this work we present the direct thermocatalytic conversion of CO2 to hydrocarbons using a novel iron nanoparticle-carbon nanotube (Fe@CNT) catalyst. We adopted a holistic and systematic approach to CO2 conversion by integrating process optimization - identifying reaction conditions to maximise conversion and selectivity towards long chain hydrocarbons and/or short olefins - with catalyst optimization through the addition of promoters, and life cycle assessment (LCA) - minimising environmental impact through catalyst and process optimization. The result is the production of valuable hydrocarbons in a manner that can approach carbon neutrality under realistic industrial process conditions.

Introduction

Fossil fuels are still predicted to contribute close to 80% of the primary energy consumption in 2040, [1] with renewable energy slowly achieving cost-parity with coal and gas. The International Panel on Climate Change predicts that staying on this course will lead to catastrophic increases in global temperatures, [2] unless further carbon dioxide emissions in the atmosphere are reduced, while renewable energy sources mature further. While efficiency gains in industrial processes and domestic consumption and carbon capture and sequestration (CCS) appear to be the main avenues to reduce emissions, [3] utilisation of CO_2 as a feedstock for chemical transformations is emerging as a complementary alternative to further support emission reduction plans across the world. Furthermore, carbon dioxide may represent an alternative feedstock to fossil fuel-derived chemicals and fuels, with a positive effect on the energy security

 [a] Dr. D. Mattia, Dr. J. O'Byrne, Dr P. Plucinski, Ms E. Sackville Department of Chemical Engineering University of Bath Claverton Down, Bath, BA27AY, UK

E-mail: d.mattia@bath.ac.uk

[b] Dr M. Jones, Dr R. Owens Department of Chemistry University of Bath Claverton Down, Bath, BA27AY, UK E-mail: m.jones2@bath.ac.uk

[c] Dr M. McManus, Dr G. Griffiths Department of Mechanical Engineering University of Bath Claverton Down, Bath, BA27AY, UK

Supporting information for this article is given via a link at the end of the document.

of most countries.[4]

A key consideration in CO₂ utilisation is to evaluate the balance between how much carbon dioxide is avoided, or offset, by converting it to chemicals and fuel and how much is produced in the process.^[5] The former is primarily related to the efficiency of the process, in terms of product distribution and feedstock conversion, determined by the catalytic route and catalyst material adopted. The latter is determined by the origin of all inputs (feedstocks and source of energy). The source of CO2, for example from flue gas of a power plant as opposed to removal from the atmosphere, has a significant impact on the capture's economic and environmental costs. Similarly, the source of hydrogen needed for CO₂ hydrogenation can dramatically affect any carbon balance, depending on the production method. The source of energy used to power the conversion process, electricity from wind as opposed to a coal power plant, will also have a major effect on the carbon balance of the entire process. Closed-loop fuel systems, where all the capture and conversion steps are powered by solar energy, appear to be promising solutions to maximise the potential for CO₂ offsets. [6]

In this work, we focus on the development of an innovative iron nanoparticle-carbon nanotube catalyst capable of operating at relatively low temperatures and producing a promising mix of hydrocarbons with industrial appeal. A full life cycle assessment of the catalyst material manufacturing and conversion process was performed. Using realistic assumptions for the sourcing of the $\rm CO_2$ and $\rm H_2$ feedstocks and the energy source for the process, [4a, 5] we show that the direct thermo-catalytic conversion of $\rm CO_2$ to hydrocarbons can approach carbon neutrality.

The Fischer-Tropsch (FT) process - the reaction of carbon monoxide with hydrogen to produce hydrocarbons - has been used industrially to produce liquid fuels since the 1920s, [7] and more recently from natural gas, and biomass syn-gas sources.[8] A wide selection of FT catalysts has been developed, based on nickel, ruthenium, cobalt and iron metal centres.[9] Iron is the preferred catalyst for feedstock compositions where hydrogen levels are low, such as that produced from coal, as it is active for both the water gas shift and the FT reaction through the formation of iron- oxides/carbides which show different activities.[10] The addition of group-2 metals, manganese and palladium among others, to iron on alumina and silica supports increases both catalyst activity and selectivity to higher order hydrocarbons. This effect has been attributed to a higher absorption of CO (and CO₂) on the catalyst surface and, hence, a higher chance of a successful coupling reaction. [11]

Carbons are often used as the catalyst support due to a higher activity per unit volume compared to other supports due to facilitated dispersion of the active species. [12] Furthermore, carbon supports tend to give higher selectivity to olefins. [13] Carbon nanotubes, in particular, are excellent candidates for heterogeneous catalysis as they are thermally stable, [14] relatively inert. [15] exhibit good adhesion for metal particles, [16]

and have low pressure drops compared to more dense silica analogues. Iron nanoparticles deposited onto CNTs via incipient wetness methods have shown to be effective FT catalysts, with the deposition method strongly affecting the catalytic performance.[17] Acid-treated CNTs were found to be effective catalyst supports for Fe nanoparticles with low deactivation rates for FT reactions.[18] Nitrogen-doped CNTs were also found to have high selectivity towards short olefins and afford long catalyst stability. [19] More recently, iron nanoparticles supported on carbon nanofibres have been used to produce short olefins with high selectivity from CO.[20] The incipient wetness method used, though, requires extensive (and energy intensive) purification steps, making it costly and with limited prospective for industrialization using CNTs as support. [21] In addition, the Fe nanoparticles have only limited contact with the CNT support, limiting the so-called hydrogen spill-over effect which has been shown to be highly beneficial in FT catalysis. [22]

In addition to the reduction in sintering, the curved CNT support surface improves H_2 spillover as a result of bridging the metal nanoparticle catalysts, which is particularly important for hydrogenation reactions.^[23] When H_2 adsorbs to a heterogeneous catalyst, direct adsorption onto the support surface is unfavourable. Bridged metal nanoparticles on the support surface provide a physical pathway for the hydrogen. The H_2 is in a lower energy state on the metal, resulting in a lower activation energy between the H_2 and the support.^[24]

The direct conversion of CO_2 to hydrocarbons has only recently started receiving attention. [4a, 25] CO_2 is first reduced in a H_2 atmosphere in the so-called reverse water-gas shift reaction (RWGS) to produce CO, followed by the FT process. Standard FT catalysts are not as effective for the conversion of CO_2 since they are designed to minimise the undesired water-gas shift reaction to increase yield. A large variety of catalysts has been tested for the direct synthesis of hydrocarbons from CO_2 , with iron giving the best selectivity away from methane - the most stable thermodynamic product — and towards higher order hydrocarbons, [4a, 25-26] or towards alcohols. [26] Minimizing methane is considered key to the economic viability of carbon utilization processes. [4]

Also important for the adoption of this technology is a process to produce the catalyst that is economic and scalable to the massive quantities required to address global carbon utilization. ^[4] In this work we developed an efficient catalyst preparation process whereby the same iron used for the synthesis of the CNTs is reactivated for CO₂ conversion with an inline mild oxidation process followed by a reduction in a hydrogen atmosphere prior to the catalytic process. ^[22] The key is to use an excess of the iron precursor which results in a large number of iron nanoparticles deposited on the surface of the CNTs. Furthermore, the catalyst particles thus formed have a large interface with the curved CNT surface, maximising hydrogen spillover. In previous publications we have shown that these catalysts, called Fe@CNT, have superior conversion and selectivity towards higher-order hydrocarbons than catalyst

prepared by the incipient wetness technique at ambient pressure. $^{[22,\ 27]}$ Here we significantly innovate on this work by adopting a holistic approach to CO_2 conversion by integrating process optimization – by identifying reaction conditions to maximise conversion and selectivity towards long chain hydrocarbons and/or short olefins, catalyst optimization – with the addition of promoters, and life cycle assessment (LCA) – by investigating the effect of catalyst and process optimization on the environmental impact of the process.

Results and Discussion

Process Optimization

Industrial FT reactors include many different designs but most are operated at moderate pressure, up to 30 bar, and temperatures below 400 °C. As such, we chose comparable pressure and temperature ranges to investigate the formation of hydrocarbons using CO2 and H2 as feedstock and the Fe@CNT catalyst in a single tube, packed bed reactor configuration. For the reaction temperature, we observed a maximum in conversion and selectivity to hydrocarbons at 370 °C for all pressures and flow rates. Once the temperature was set, the optimal flow rate was found to be 8 sccm (1:3 CO2:H2) above which selectivity to methane increases. Under these conditions, we found that performing the catalyst reduction step under an atmosphere of hydrogen at 5 bar afforded the optimum conversion and selectivity (see experimental section for further details on catalyst activation). Finally, with temperature, flow rate and reduction pressure set as discussed above, we observed an increase in overall conversion with increasing reaction pressure, with maximum total hydrocarbon conversion at 2.5 bar but highest selectivity to higher order hydrocarbons at 7.5 bar. All data is reported in Fig.1 and values for each experiment are reported in Fig. S1 in the supplementary section. Although a significant amount of methane is still produced (about 30%), the optimal process conditions showed a promising olefin/paraffin ratio, particularly for shorter ones (C2-C4= {alkenes} vs. C2-C4 {alkanes}) while still producing longer hydrocarbons (C5+ {all

Stability and re-usability of the catalyst at 7.5 bar was also investigated, showing good results for both (Fig. 2). This compares well with FT-only iron-carbon nanofibre, [20] and Fe-CNT catalyst. [17] Nonetheless, the present results are still far away from the stability of commercial FT-only catalysts. [7] Repeating the hydrogen reduction step in line can partially regenerate the catalyst, [27] while we noticed a decrease in HC conversion and selectivity towards long hydrocarbons when catalyst reactivation was carried out after the catalyst was left on the shelf in air for several days between reactions.

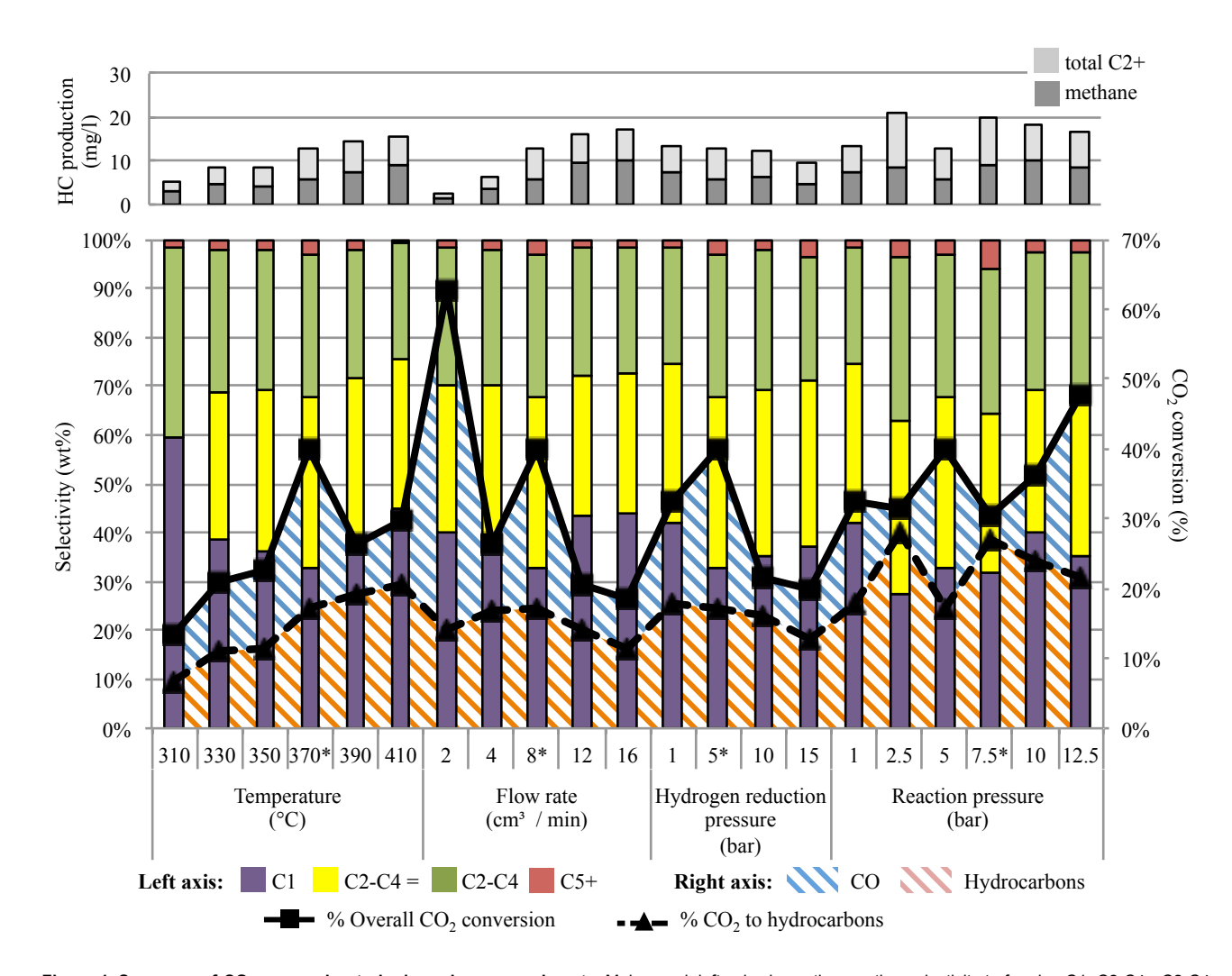


Figure 1. Summary of CO_2 conversion to hydrocarbons experiments: Main panel, left axis shows the reaction selectivity to forming C1, C2-C4₋, C2-C4, and C5+ hydrocarbons; the right axis shows the overall CO_2 conversion and the percentage of CO_2 converted to hydrocarbons (excluding carbon monoxide). The top panel shows the split between methane and C2+ hydrocarbons.

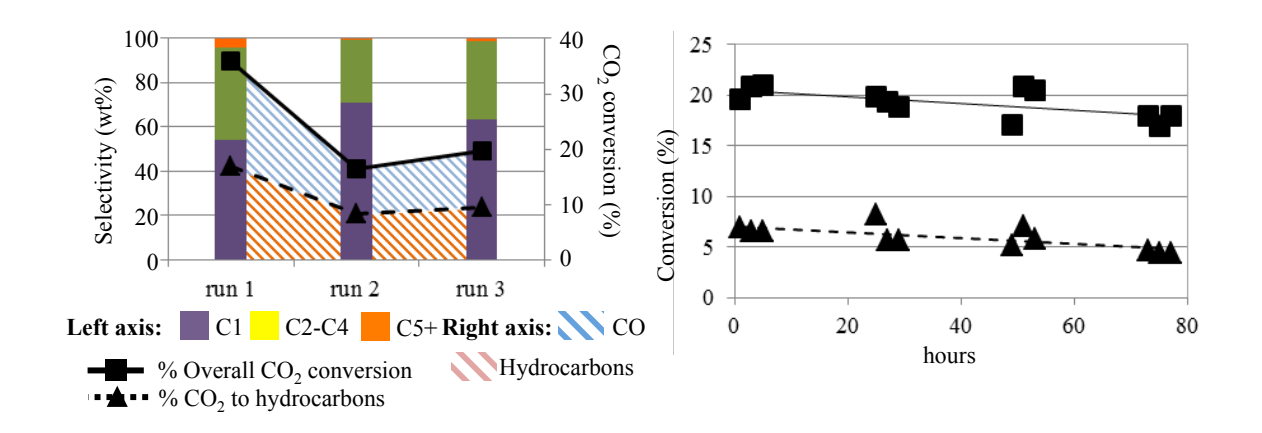


Figure 2. Stability and re-usability tests: Left: selectivity and conversion for three 4-hour runs using the same Fe@CNT catalyst batch under the same catalyst conditions. Right: 3-day continuous run for the same Fe@CNT catalyst.

Catalyst Optimization and Promoter Addition

From the analysis of data in Fig. 1, the optimal reaction conditions, maximising hydrocarbon production while at the same time minimising the production of methane were identified as 370 °C for the temperature, 8 sccm for the flow rate, 5 bar for the pressure of the *in line* hydrogen reduction prior to performing the reaction and 7.5 bar for the reaction pressure. We then proceeded to investigate the effect of the addition of promoters including alkali and platinum group metals that have shown to improve conversion and selectivity for the FT reaction.^[11] All data is reported in Fig. 3 and values for each experiment are reported in Fig. S2 in the supplementary section.

The addition of alkali metals also shifts selectivity towards olefins and C5+ hydrocarbons. The latter effect is well-known in the literature for Fe-based FT catalysts. [26] The selectivity towards olefins is kept up to C7 hydrocarbons (Fig. 4). These

are of interest for a variety of industries, from jet fuel production to monomers, solvents and detergents. [26, 28] Cs has marginally better selectivity and overall conversion than Na, though the latter is more readily available. K has lower HC yield and slightly higher selectivity towards methane, somewhat in disagreement with what observed for traditional Fe-based FT catalysts. [29] The addition of palladium as a promoter produced a significant increase in HC yield and total conversion, but shifted selectivity towards methane. This result is in contrast with previous investigations showing a beneficial effect of the addition of palladium as a promoter to iron-silica systems, [28] and can probably be attributed to the different support material. Calcium and magnesium produce almost exclusively methane. Despite numerous examples where Mn has acted as a promoter for the conversion of CO₂ to hydrocarbons, [11b, 26] when 0.5 wt % Mn was added to the Fe@CNTs the results were significantly worse.

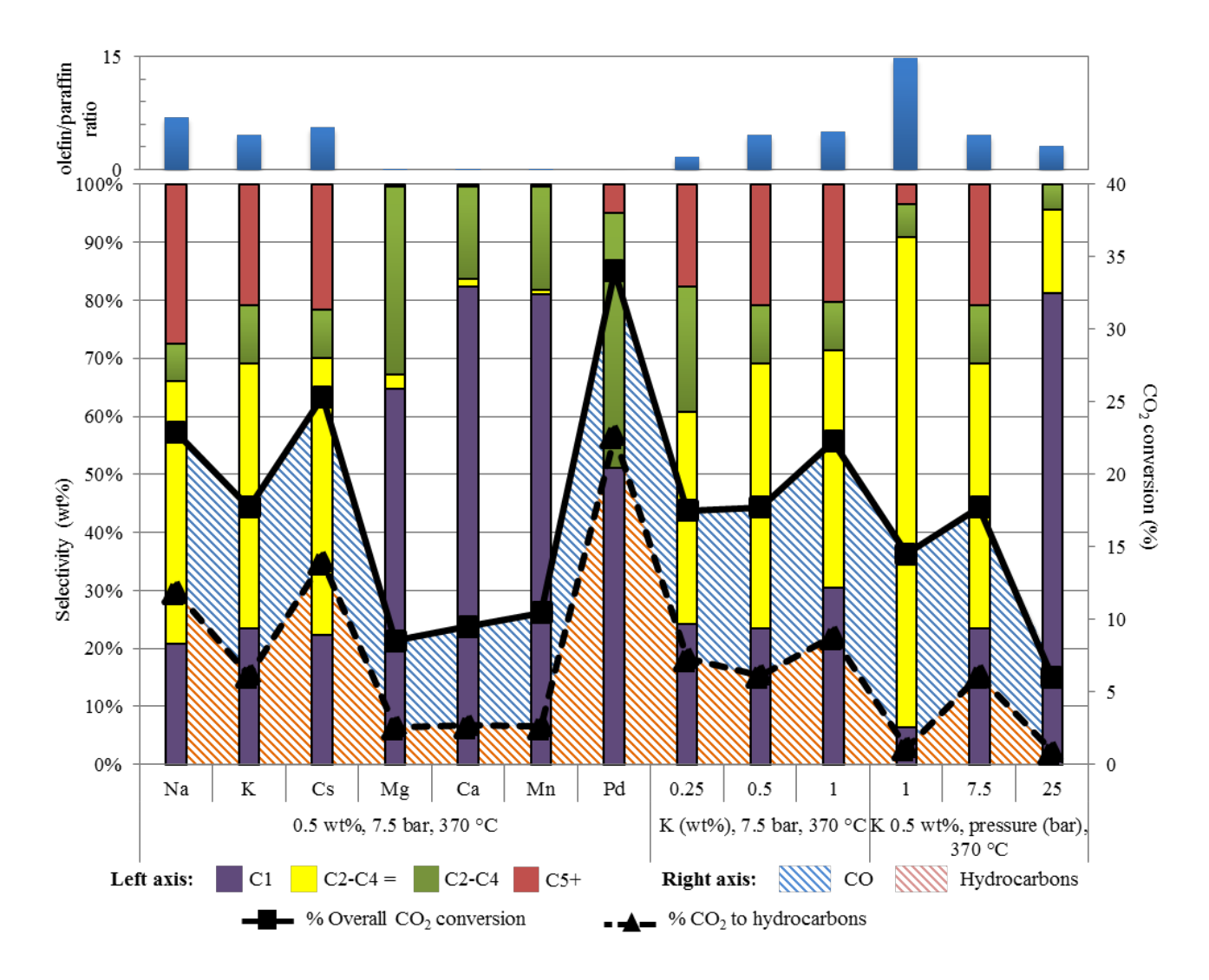


Figure 3. Summary of CO_2 conversion to hydrocarbons in presence of promoters: Main panel, left axis shows the reaction selectivity to forming C1, C2-C4=, C2-C4 and C5+ hydrocarbons; the right axis shows the overall CO_2 conversion and the percentage of CO_2 converted to hydrocarbons (excluding carbon monoxide). The top panel shows the olefin / paraffin ratio.

In addition to poor selectivity to long-chain hydrocarbons, the conversion dropped by about a third, from 40% with Fe@CNTs to 10% with the addition of the Mn promoter. A review of the literature shows that whenever manganese has been used successfully as a promoter, it was in the role of co-catalyst, often with potassium as well as iron. [11b, 30] It is therefore not unreasonable to suggest that the improvements observed by other groups are as a result of the second metal, either alone or in conjunction with the manganese, rather than the manganese alone.

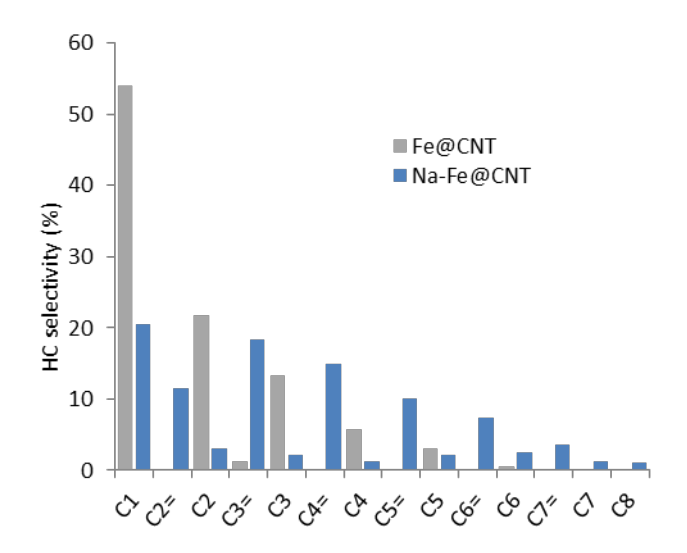


Figure 4. Olefin/paraffin selectivity: the addition of sodium to the Fe@CNT catalyst induces a significant shift towards higher selectivity for short olefin production compared to the un-promoted base catalyst. Results for the sodium as a promoter are representative for potassium and caesium as well.

Life Cycle Assessment

Although the production of valuable hydrocarbons from CO2 could represent a sufficient economic incentive for large emitters to capture the CO₂ in the first place, [4a] its potential for mitigating the effects of global warming is not guaranteed, as energy and additional resources are needed to capture and convert the emitted CO2 into a useful product. [5] A detailed life cycle assessment (LCA) along with the elaboration of several realistic scenarios is reported here (the scope of which includes the capture stage). We start from considering the laboratory process used for this work and the un-promoted Fe@CNT catalyst: The incurred impacts of all aspects of the process have been considered, from the synthesis of the catalysts and of the feedstock gases to the infrastructure (electricity using current UK grid mix and all reactor and furnace materials) to the energy needed to heat the laboratory furnace. A detailed analysis and description of methodology used here can be found elsewhere. [21, 31] The term 'offset' used in this paper includes all the processes and supply chains, and their resultant GHG outputs that would be avoided by using this process. This can also be thought of as an 'avoided impact'.

As can be seen in the first two columns of Fig. 5, the laboratory process offsets less than 1% of CO₂ used (note that the y-axis is

in logarithmic scale). This means the process is generating about 100 times more CO_2 than it consumes. This is expected, as the laboratory process is not optimized nor designed to minimize emissions.

The study shows the life cycle impact of the process under a number of differing scenarios, using LCA as a development tool to investigate the transition research from the laboratory to large scale. [32] The data in the second set of columns (Fig. 5) has been modelled under realistic (and conservative) assumptions to extrapolate the behaviour of a hypothetical large-scale, industrial version of this process. First, we analyse the significant contribution to the LCA due to the heating of the laboratory furnace: The laboratory furnace used has an overall efficiency of less than 1%, due to its design focused on providing fast heating rates and to the fact that the large amount of heat generated is lost to the environment. In a large-scale, continuous operation, after the start-up phase, the heat generated during the reaction due to its exothermic nature would be recovered and used either in secondary processes or used to pre-heat the feeds to the reactor itself. Offsets using heat recovery are modelled as the electricity that can be produced from power generators utilizing the heat for electricity production, thus offsetting current UK electricity grid mix, as detailed later in the experimental section. The second set of columns, therefore, does not include the impact generated to heat the laboratory furnace. Furthermore, the impacts arising from the catalyst synthesis are optimized for a continuous manufacturing process, as reported elsewhere. [21] Still, the process is producing more CO2 that it offsets. The third set of columns considers a more favourable, low carbon, energy mix, from a EU representative large scale wind power operation, [33] producing only 10 g CO₂/kWh, compared to 540 g CO₂/kWh for the UK grid mix.^[34] It is noted here that these are the full cycle values, not just stack emissions, i.e. they also include all upstream processing, e.g. mining, refining, distilling etc. This affects the infrastructure impacts considered. Naturally, a different grid mix would produce different results. In this scenario, the un-promoted Fe@CNT catalyst process would be offsetting about 45% of the CO2 produced, still emitting more CO₂ than is consumed.

The scenarios above are all based on the use of a single reactor tube, as in the laboratory case. Commercial FT reactors like the ARGE reactor pioneered by Sasol in the 1960s, use multi-tube (up to 2,500) packed-bed reactors in a tube-and-shell configuration for optimal heat dissipation.[35] A multi-tube reactor configuration compared to our single one will see a significant reduction in thermal duty as the surface-to-volume ratio improves dramatically and the design is optimized. Based on the experimental data of the present work, a 40% reduction in infrastructure costs would be needed to achieve a carbon neutral scenario, as reported in the fourth set of columns in Fig 5. While the number above is sizeable, it is noted that the ARGE design is the oldest and least efficient of current FT reactor designs, with modern slurry-based reactors having ~40% lower construction costs than the ARGE one,[7] which will translate in a reduction of infrastructure emissions. Furthermore, as discussed in the experimental section, heat recovery from exothermic systems can reach efficiencies close to 50%. Therefore we

consider this assumption a reasonable and conservative one. For example, if one were to consider a 60% reduction in

infrastructure emissions (rather than 40%), there would be a net reduction of CO_2 of about 40%.

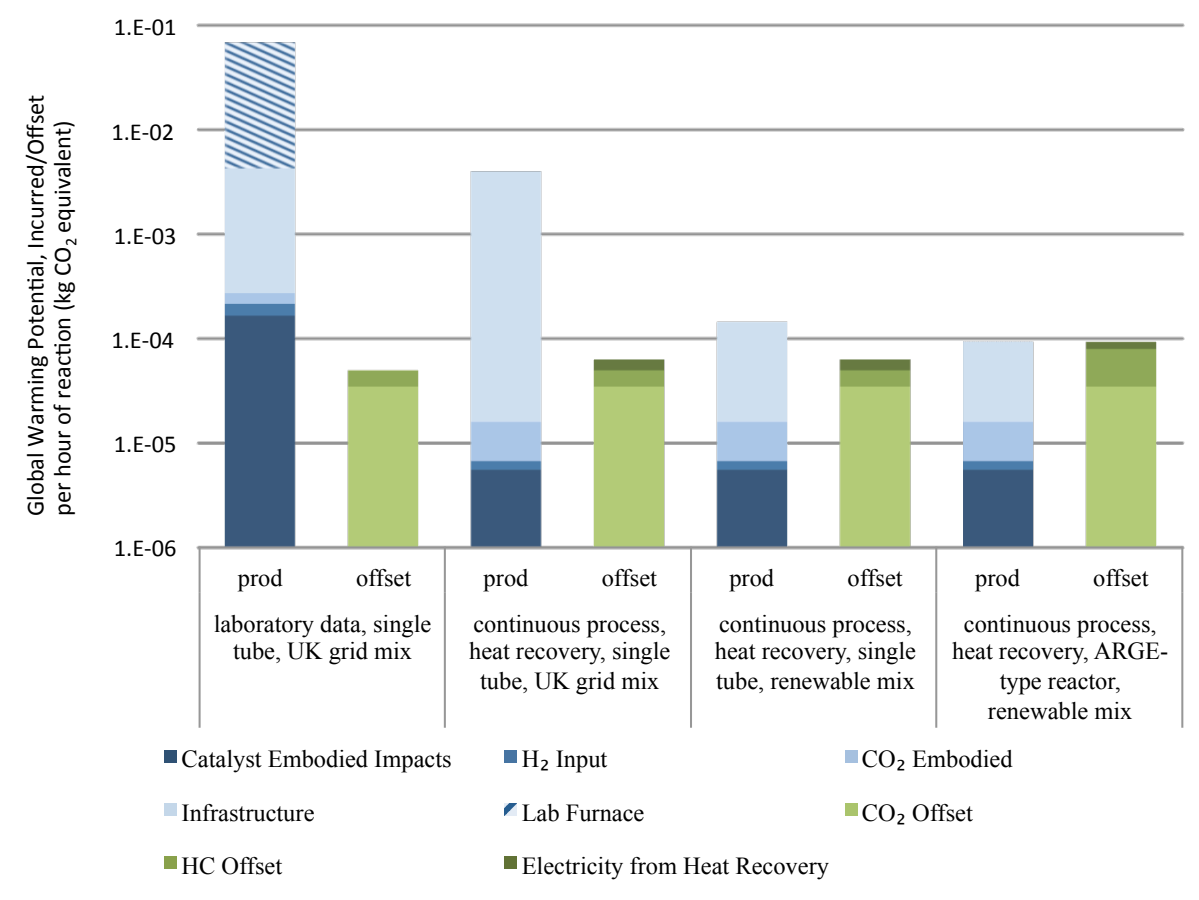


Figure 5. LCA of the CO₂ conversion process using the Fe@CNT catalysts: The first set of columns reports the raw data for the laboratory process using a single tube reactor for the un-promoted catalyst (reaction conditions: 2.5 bar, 370 °C); the second set refers to a continuous industrial process where the exothermic heat of reaction is recovered; the third set of columns considers the effect of using a renewable energy mix rather than the UK grid one; the final set of columns considers a carbon neutral case obtained by assuming a 40% reduction in infrastructure impacts. This scenario is based on using a multi-tube reactor, modelled on the ARGE reactor developed by Sasol.

Promoter Addition

The addition of the promoters to the catalyst synthesis process significantly increases the offsets due to the increased conversion and selectivity towards lower olefins and away from methane, but at the same time increases the catalyst embodied impacts (Table 1), resulting in a modest improvement in the offset compared to the un-promoted catalyst (third set of columns in Fig.5). There is no simple relation between the offset and hydrocarbon chain length as, for example, formation of isoand n-butane generates a higher offset than propane or hexane. The specific offset values for each HC produced can be found in Fig. S3 in the supplementary data section.

The catalyst with the potassium promoter has a lower offset given by hydrocarbon production compared to the other two promoters due to a combination of a lower overall conversion to HC and higher methane production. The increase in catalyst embodied impact for the three promoters is similar and due to the synthesis method of the promoter precursor (e.g. the Solvay

process for the sodium bicarbonate). Identifying an alternative method to add the promoters that uses a more sustainable process could allow reaping the environmental benefits of the promoters improving both HC conversion and selectivity.

Table 1. Effect of promoter addition on catalyst embodied impact and offset from hydrocarbon production. Reaction conditions: 7.5 bar, 370 °C, 0.5wt% promoter..

Catalyst	Catalyst embodied impact	Offset from HC production	Total offset (%)
Fe@CNT	6.43E-06	1.97E-05	50
Na-Fe@CNT	1.18E-05	2.95E-05	50
K-Fe@CNT	1.18E-05	1.43E-05	25

Conclusions

In this work we have discussed a novel iron nanoparticle-carbon nanotube (Fe@CNT) doped catalyst material for the direct conversion of CO2 to hydrocarbons. Reaction temperature, pressure and feed gas flow rate were optimized to maximise conversion and selectivity towards (valuable) long chain HCs and/or short olefins. The addition of promoters (particularly alkali metals) further improved both, particularly shifting selectivity away from methane and significantly increasing the olefin/paraffin ratio up to C7 hydrocarbons. The catalyst optimization process was augmented by a comprehensive life cycle assessment study of all the process impacts, from sourcing of all materials to offsets of the produced HCs. Results show the overwhelming importance of the energy source needed for the thermo-catalytic conversion process and the necessary steps that would be required, under realistic (and conservative) industrial conditions the process, using the Fe@CNT catalyst to move towards a carbon neutral system.

Experimental Section

Fe@CNT catalyst production

The preparation of the Fe@CNT catalyst has been described in detail elsewhere. [22, 27] Briefly, a solution of ferrocene in toluene is injected at high temperature inside a furnace at 790 °C under 450 sccm Ar and 50 sccm H2 in a quartz tube filled with quartz beads (added to increase yield). Due to the stoichiometric excess of ferrocene, the CNTs formed contain a high density of iron metal nanoparticles embedded on their walls as well as inside the tubes' bore. [27] The iron nanoparticles are not accessible in the as-produced samples as they are coated with a graphitic carbon layer. In previous publications we have shown that this graphitic layer can be removed with oxidation in air at 570 °C without damaging the supporting CNTs and with the transformation of the metallic iron to iron oxide, primarily $\text{Fe}_2\text{O}_3.^{\text{[22, 27]}}$ Subsequent reduction under a H₂ atmosphere partially reduces the iron, making it catalytically active producing what have been termed Fe@CNTs (Fig. 6). The formed iron nanoparticles are moulded on the surface of the nanotube, ensuring a higher contact surface than the incipient wetness case.

Promoter Addition

A range of metal promoters was added to the as-produced CNTs (before activation in air) via incipient wetness. Due to the range of compounds used as metal sources, two slightly different procedures were used (Table 2). In the first instance, methanol was used as a solvent. The desired weight loading was calculated with regards to the metal, and was dissolved in ~5 ml methanol. The resultant solution was added to 0.5 g Fe@CNTs, and a further 10 ml methanol was added to aid dispersion. The emulsion was stirred for 24 hours at room temperature, after which time the methanol had evaporated. When the metal compound was insoluble in methanol (i.e. when the metal source was from a carbonate),

water was used as the solvent. The procedure was the same as with methanol until the evaporation step. In order to aid evaporation, the solution was heated to ~100 °C for an hour to fully remove the water. No significant difference was observed between the two procedures and the resulting materials. Raman of the K-Fe@CNT showed no peak for the carbonate (with an active band at 1066 cm^{-1}), [36] and no difference with the Fe@CNT (Fig. S4). The result for the K-Fe@CNT is representative for the other promoters as well.

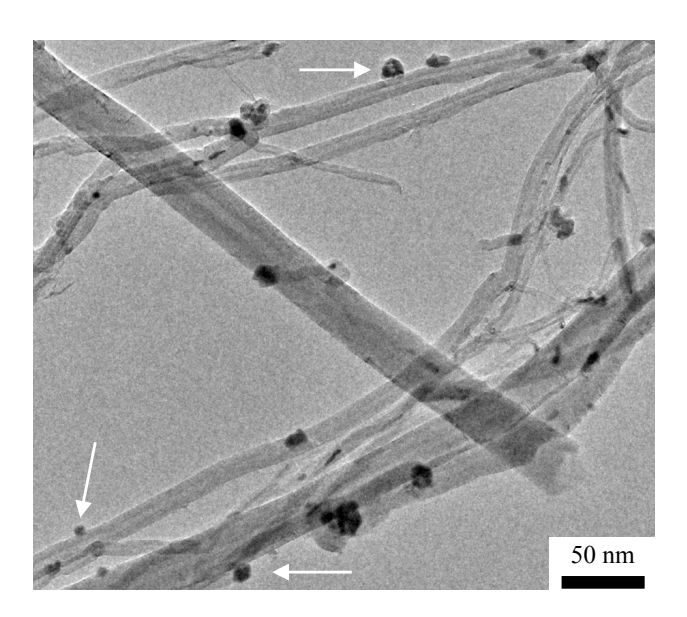


Figure 6. TEM Characterization: TEM micrograph (Jeol 2100F) of Na-Fe@CNT, after activation but before catalytic testing, showing the presence of iron/iron oxide nanoparticles on the surface of the CNTs.

Table 2. Metal sources and relative solvents for the different promoters added to the Fe@CNT base catalysts

Catalyst	Promoter (0.5 wt% a Fe@CN	solvent	
	source	amount (mg)	
K-Fe@CNT	KHCO₃	6.4	water
Na-Fe@CNT	NaHCO ₃	9.3	water
Cs-Fe@CNT	Cs ₂ CO ₃	3.0	water
Pd-Fe@CNT	Pd(OAc) ₂	5.0	methanol
Ca-Fe@CNT	Ca(NO ₃) ₂ .4H ₂ O	15.0	methanol
Mg-Fe@CNT	$Mg(NO_3)_2.6H_2O$	26.0	methanol
Mn-Fe@CNT	Mn(OAc) ₂ .2H ₂ O	12.2	methanol

Catalyst activation and characterization

The resulting promoter-Fe@CNTs were thermally oxidised at 560 $^{\circ}$ C for 30 minutes and then reduced *in line* under a 1 bar hydrogen atmosphere for 3 hours at 400 $^{\circ}$ C prior to the catalytic experiment, as previously discussed. [22]

The presence of sodium in a Na-Fe@CNT sample was observed via XPS of samples before and after catalytic testing with no noticeable differences (Fig. S5). No difference in the sodium peak was observed, whereas differences in the iron peaks have been discussed in previous publications, with the formation of mixed iron/iron oxide/iron carbide structures. [27] Raman of the Fe@CNT before and after catalytic testing showed no noticeable difference (Fig. S6). Analysis of the effect on the un-promoted catalyst of repeated catalytic testing is reported elsewhere. [22, 27] SEM micrographs and EDS analysis (JEOL FESEM6301F + Oxford ISIS) of Na-Fe@CNT after activation but before catalytic testing show (qualitatively) a relatively uniform distribution of the promoter, also with the presence of small metal clusters due to imperfect dispersion (Fig. 7). These results are representative for the other promoters investigated.

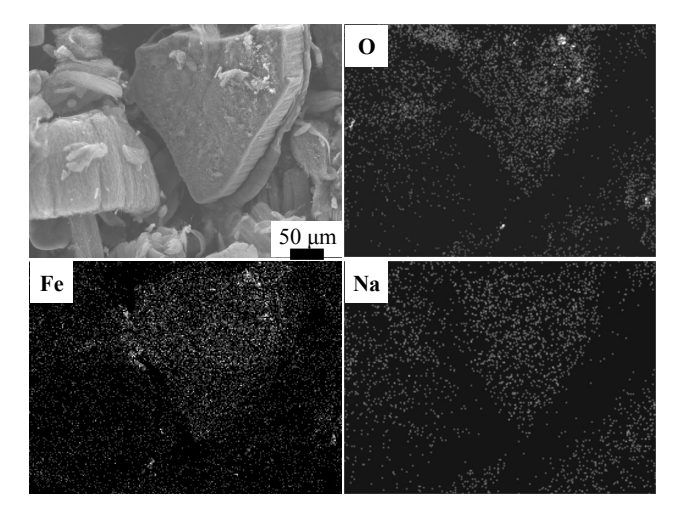


Figure 7. SEM/EDS Characterization: SEM micrograph and EDS elemental mapping for a Na-Fe@CNT sample. The SEM micrograph shows a typical nanotube sample produced during CVD on the surface of the quartz support. The elemental mapping shows a uniform distribution of the sodium, despite the much weaker signal compared to iron due to the lower concentration and molecular weight. Elemental maps have the same scale as the micrograph.

Catalytic testing

The activity of each catalyst was tested using a 1 cm diameter packed bed, stainless steel reactor with ca. 0.4~g of catalyst, giving a bed length of ca. 5~cm in the centre of the reactor. The catalyst was secured in place with high temperature glass wool (15 cm at the exit, 10 cm at the entrance). Unless otherwise specified, reaction conditions were as follows: 3~bour hydrogenation step at 400~°C with a continuous flow of hydrogen (20~sccm) at 5~bar; reaction was conducted at 370~°C, 7.5~bar, with a flow of CO_2 and H_2 in a 1:3~ratio (2~sccm and 6~sccm respectively).

Samples were taken every hour using an air-tight gas syringe (30 ml), and the product mixture was analysed using an Agilent 7890A GCMS with a HP-PLOT/Q, 30 m long, and 0.320 mm diameter column. A BOC calibration mixture containing 1 % v/v CH₄, C_2H_6 , C_3H_8 , C_4H_{10} , CO and CO₂ with a N₂ makeup gas was used for each experiment to calibrate the GCMS.

Life Cycle Assessment

This LCA work covers the impacts associated with the operation and upstream emissions of the processes involved in the production of hydrocarbons via the RWGS-FT process, i.e. all stages necessary in the formation of the obtained gaseous and liquid products of the reactions. The system boundary for this process can be considered a cradle-to-gate assessment, as shown in Fig. 8. It includes all catalyst and feedstock embodied impacts, including their in-use and regeneration phases; all infrastructure impacts including source materials for apparatus and electricity.

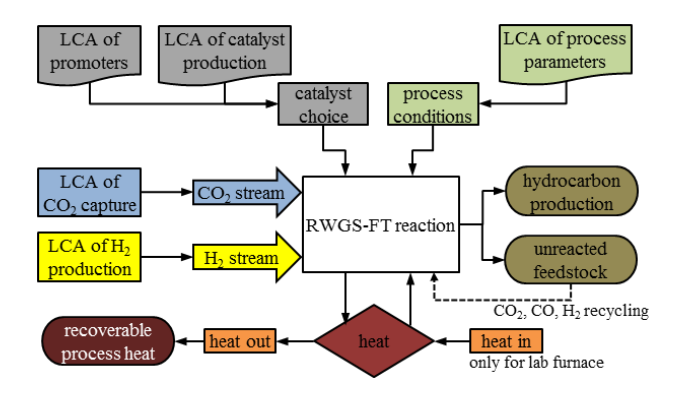


Figure 8. Overview of LCA inputs and outputs.

The catalytic conversion process has been assessed relative to existing published manufacturing routes of the hydrocarbon species, which are fossil fuel based, with data sourced from the Ecoinvent life cycle inventory. [31b]

The process inputs are weighted across a predicted 5000 h catalyst operational lifetime, with the functional unit (FU) being kilograms of formed hydrocarbons, kgHCs. The FU is a combined measure of the C1 to C7 HC species formed. The allocation of impacts is assessed on a mass basis. The greenhouse gas (GHG) values, presented in kilograms of CO_2 equivalent emissions, are calculated using the IPCC GWP 100a environmental impact assessment methodology. $^{[2]}$ It is important to note that these GHG figures are cradle-to-gate impact, and are presented within the boundaries of sourcing, refining, and bringing the hydrocarbon product to the point of use and not the GHG impacts of the release of these products. The latter would be identical independent of the source and method of the specific HC production route.

Material and chemical inputs

The chemical compound database PubChem34 allowed the most common manufacturing routes of all the chemicals used in the research to be established. PubChem along with Ullmann's Encyclopaedia^[37] were used to confirm that the datasets located in the Ecoinvent life cycle inventory database^[38] were representative, and sufficiently accurate for the LCA.

Catalyst embodied Impacts and promoter addition

The catalyst embodied impacts are the product of the respective quantity of CNT used in addition to the impacts of the different promoter materials added to the respective catalysts.^[21, 31a]

The assessment comprises of a stoichiometric analysis of all promoter materials, including precursor chemicals, in addition to modelling all necessary stages from initial ore extraction to final purified promoter compounds introduced onto the CNT surface and activated ready for the catalysis process.

Sodium bicarbonate was modelled on the further addition of CO_2 to its carbonate precursor, dataset within Ecoinvent. Potassium bicarbonate inventory founded upon relevant literature, $^{[39]}$ as reported in Table 1. With no data present for caesium in the LCA literature, an assumption has been taken that Caesium carbonate will very likely exhibit similar environmental footprint to that of potassium carbonate, since both are formed via a similar process.

Laboratory Infrastructure Contribution

The equipment used for the laboratory experiments is not optimized for energy and impact minimisation compared to a large-scale industrial process. However, the laboratory equipment was fully assessed in the analysis, providing an indicative account of likely LCA impacts of the different process operations required to produce the catalysts and the hydrocarbon products. The LCA study also included the component parts and material construction of the different equipment, based on manufacturer technical specifications. Datasets on the major component parts made from metals, plastics, rubbers, ceramics, and electronic components were also taken from EcoInvent. [38] The precise methodology used can be found in ref. [21, 31]

Heat Recovery

Similarly to the infrastructure contribution, the laboratory setup requires continuous provision of heat energy to operate, whereas in Fischer-Tropsch plants, heat is generated due to exothermic nature of the reaction and recovered, [40] using water/steam as the process fluid, which in turn can be used for power generation. [41] Using the Carnot cycle to calculate the maximum amount of work recoverable by a heat engine operating between the reaction process temperature and ambient one obtain a maximum of ~54 %. Since steam turbines have efficiency in 70-90% range, the obtainable overall energy from the process is calculated to be closer to 48%. A model to evaluate the amount of obtainable heat available from the Fischer-Tropsch process, considering the product distribution and amount formed, for CO as feedstock, [42] has been adapted for CO₂ as a feedstock. [31b] Considering the achievable efficiencies, and theoretical heat provision, the produced electricity is approximated to be 1.19 kWh per kilogram of FT product. This electricity generation approximation, in conjunction with the dataset produced for the UK electricity grid mix, allows the avoided emissions of generation via the recovery of waste heat to be calculated.

Assumptions for optimized process

The adopted 'lean' laboratory setup and other process enhancement measures include:

- Enhanced operational efficiency, during catalyst synthesis and operation, represented by laboratory equipment being used to full capacity, and no ramp-up, ramp-down or idle periods.
- The supply of hydrogen is modelled on a hypothetical process using electricity derived from wind power for the electrolysis of seawater; adapted from Ecoinvent dataset of a membrane cell.^[43]
- -The palladium catalyst embodied impacts are further lowered by an end-of-life recovery of 70% of the precious metal via an acid dissolution stage. $^{[31b]}$
- A feedstock gas recycling loop is hypothesised, whereby the impacts attributable to the use of the H_2 and CO_2 reactant gases are significantly minimised, since unreacted gas is considered to be available for subsequent re-use and catalyst bed passes.

Sensitivity to selectivity and modelling datasets used for the produced hydrocarbons

Representative life cycle dataset for methane is Natural Gas extracted from a UK offshore facility and piped to the mainland, whereas other hydrocarbons are distillates of a petrochemical refinery. Therefore, having a bias, or selectivity, towards longer-chained hydrocarbons but with a lower yield, can result in greater offsets than catalysts with higher yields but of the less environmentally beneficial product. [31a]

The LCA outcomes would strongly enforce the drive to produce catalysts with a lesser tendency towards methane production. This statement, however, is dependent on the chosen source of methane to be offset: From the LCA datasets used (Ecoinvent Database v2.2) methane from natural gas routes is between 25 and 90 times less impactful than the routes for other C2-C7 hydrocarbons being produced. Bio-methane, for example, was approximately found (Ecoinvent Database v2.2) to be 80 times more impactful than natural gas, in this there would be at the very least little penalty and some cases a positive benefit for the production of methane over all other hydrocarbons. The more conservative and less favourable option was chosen here.

Acknowledgements

The authors wish to acknowledge the EPSRC (grant EP/H046305/1 and EP/G03768X/1) and the University of Bath (CSCT, Bath Ventures and HEIF funding).

All data created during this research is available in the online supplementary document.

Keywords: carbon dioxide utilisation • carbon nanotubes • Fisher-Tropsch • iron nanoparticle catalyst • carbon utilisation

- [1] Annual Energy Outlook, EIA, 2014.
- [2] International Panel on Climate Change, 4th Assessment Report, 2007.
- [3] R. Monastersky, in *Nature, Vol. 504*, Nature, **2013**, pp. 339–340

[4]	aG. Centi, E. A. Quadrelli, S. Perathoner, <i>Energy & Environmental Science</i> 2013 , <i>6</i> , 1711-1731; bM.	[25]	W. Wang, S. P. Wang, X. B. Ma, J. L. Gong, <i>Chem. Soc. Rev.</i> 2011 , <i>40</i> , 3703-3727.
	Aresta, A. Dibenedetto, <i>Dalton Transactions</i> 2007 , 2975-2992.	[26]	R. W. Dorner, D. R. Hardy, F. W. Williams, H. D. Willauer, <i>Energy & Environmental Science</i> 2010 , <i>3</i> ,
[5]	N. von der Assen, J. Jung, A. Bardow, <i>Energy</i> &		884-890.
	Environmental Science 2013.	[27]	D. R. Minett, J. P. O'Byrne, S. I. Pascu, P. K. Plucinski,
[6]	aD. Marxer, P. Furler, J. Scheffe, H. Geerlings, C.		R. E. Owen, M. D. Jones, D. Mattia, <i>Catalysis Science</i>
	Falter, V. Batteiger, A. Sizmann, A. Steinfeld, <i>Energy Fuels</i> 2015 , <i>29</i> , 3241-3250; bP. Furler, J. R. Scheffe, A.	[28]	& Technology 2014 , 3351-3358. R. E. Owen, J. P. O'Byrne, D. Mattia, P. Plucinski, S. I.
	Steinfeld, Energy & Environmental Science 2012, 5,	[20]	Pascu, M. D. Jones, <i>ChemPlusChem</i> 2013 , <i>78</i> , 1536-
	6098-6103.		1544.
[7]	H. Schulz, <i>Appl. Catal. A-Gen.</i> 1999 , <i>186</i> , 3-12.	[29]	M. Luo, W. Shafer, B. Davis, Catal. Lett. 2014, 144,
[8]	M. E. Dry, Catal. Today 2002 , <i>71</i> , 227-241.		1031-1041.
[9]	E. de Smit, B. M. Weckhuysen, Chem. Soc. Rev. 2008,	[30]	M. L. Cubeiro, G. Valderrama, M. R. Goldwasser, F.
[10]	37, 2758-2781. E. S. Lox, G. F. Froment, <i>Ind Eng Chem Res</i> 1993 , <i>32</i> ,		González-Jiménez, M. C. Da Silva, M. J. Pérez-Zurita, in Stud. Surf. Sci. Catal., Vol. Volume 107 (Eds.: R. L.
[10]	71-82.		E. C. P. N. J. H. S. M. de Pontes, M. S. Scurrell),
[11]	aP. S. Sai Prasad, J. Bae, KW. Jun, KW. Lee, Catal		Elsevier, 1997 , pp. 231-236.
[]	Surv Asia 2008 , <i>12</i> , 170-183; bR. W. Dorner, D. R.	[31]	aO. G. Griffiths, R. E. Owen, J. P. O'Byrne, D. Mattia,
	Hardy, F. W. Williams, H. D. Willauer, App Catal A:		M. D. Jones, M. C. McManus, RSC Advances 2013, 3,
	General 2010 , 373, 112-121.		12244-12254; bO. G. Griffiths, University of Bath 2014 .
[12]	B. Sun, K. Xu, L. Nguyen, M. H. Qiao, F. Tao,	[32]	A. Hetherington, A. Borrion, O. Griffiths, M. McManus,
[42]	Chemcatchem 2012 , 4, 1498-1511.	[22]	Int J Life Cycle Assess 2014, 19, 130-143.
[13]	E. van Steen, F. F. Prinsloo, <i>Catal. Today</i> 2002 , <i>71</i> , 327-334.	[33]	Varun, I. K. Bhat, R. Prakash, Renewable and Sustainable Energy Reviews 2009, 13, 1067-1073.
[14]	Y. A. Kim, H. Muramatsu, T. Hayashi, M. Endo, M.	[34]	UK Department of Energy & Climate Change, 2011 .
1	Terrones, M. S. Dresselhaus, Chem. Phys. Lett. 2004,	[35]	J. J. McKetta, Supercritical Fluid Technology: Theory
	398, 87-92.		and Application to Technology Forecasting, Vol. 56,
[15]	F. Rodríguez-reinoso, <i>Carbon</i> 1998 , 36, 159-175.		1996.
[16]	G. G. Wildgoose, C. E. Banks, R. G. Compton, Small	[36]	I. Martinez, C. Sanchez-Valle, I. Daniel, B. Reynard,
[17]	2006 , 2, 182-193. M. C. Bahome, L. L. Jewell, D. Hildebrandt, D. Glasser,	[37]	Chem. Geol. 2004 , 207, 47-58. ULLMANN'S Encyclopedia of Industrial Chemistry,
[17]	N. J. Coville, <i>Appl. Catal. A-Gen.</i> 2005 , 287, 60-67.	[37]	online edition ed., Wiley.
[18]	R. M. M. Abbaslou, A. Tavasoli, A. K. Dalai, <i>Appl.</i>	[38]	Griffiths OG. Environmental Life Cycle Assessment of
	Catal. A-Gen. 2009 , 355, 33-41.		Engineered Nanomaterials in Carbon Capture and
[19]	H. J. Schulte, B. Graf, W. Xia, M. Muhler,		Utilisation Processes: PhD Thesis,
1001	ChemCatChem 2012, 4, 350-355.	1001	http://opus.bath.ac.uk/41318/, University of Bath; 2014.
[20]	H. M. Torres Galvis, J. H. Bitter, C. B. Khare, M.	[39]	H. Schultz, G. Bauer, E. Schachl, F. Hagedorn, P.
	Ruitenbeek, A. I. Dugulan, K. P. de Jong, <i>Science</i> 2012 , <i>335</i> , 835-838.		Schmittinger, in <i>Ullmann's Encyclopedia of Industrial Chemistry</i> , Wiley-VCH Verlag GmbH & Co. KGaA,
[21]	O. G. Griffiths, J. P. O'Byrne, L. Torrente-Murciano, M.		2000.
[]	D. Jones, D. Mattia, M. C. McManus, <i>Journal of</i>	[40]	B. Davis, <i>Top Catal</i> 2005 , 32, 143-168.
	Cleaner Production 2013, 42, 180-189.	[41]	B. Jager, R. Espinoza, <i>Catal. Today</i> 1995 , 23, 17-28.
[22]	J. P. O'Byrne, R. E. Owen, D. R. Minett, S. I. Pascu, P.	[42]	P. Chaumette, C. Verdon, P. Boucot, <i>Top Catal</i> 1995 ,
	Plucinski, M. D. Jones, D. Mattia, Catalysis Science &		2, 301-311.
[23]	Technology 2013, 3, 1202-1207. S. K. Beaumont, S. Alayoglu, C. Specht, N. Kruse, G.	[43]	HJ. Althaus, G. Doka, R. Dones, T. Heck, S. Hellweg, R. Hischier, T. Nemecek, G. Rebitzer, M. Spielmann,
ردع	A. Somorjai, <i>Nano Lett.</i> 2014 , <i>14</i> , 4792-4796.		G. Wernet, (Eds.: R. Frischknecht, N. Jungbluth),
[24]	R. Prins, <i>Chemical Reviews</i> 2012 , <i>112</i> , 2714-2738.		2007 .
	, , , , , , , , , , , , , , , , , , , ,		

